Hindawi Publishing Corporation
Journal of Nanomaterials
Volume 2014, Article ID 104136, 7 pages
http://dx.doi.org/10.1155/2014/104136

Research Article

Improvement of Short-Circuit Current Density in p-$Ni_{1-x}O$:Li/n-Si Heterojunction Solar Cells by Wet Chemical Etching

Feng-Hao Hsu,[1] Na-Fu Wang,[2] Yu-Zen Tsai,[2] Ming-Hao Chien,[2] and Mau-Phon Houng[1]

[1] *Department of Electrical Engineering, Institute of Microelectronics, National Cheng Kung University, No. 1 Dasyue Road, East District, Tainan City 701, Taiwan*
[2] *Department of Electronic Engineering, Cheng Shiu University, 840 Chengcing Road, Niaosong District, Kaohsiung City 833, Taiwan*

Correspondence should be addressed to Mau-Phon Houng; mphoung@eembox.ncku.edu.tw

Received 15 June 2014; Accepted 26 August 2014; Published 21 September 2014

Academic Editor: Chien-Jung Huang

This study confirms that the surface texturation of window layer (Al-Y codoped ZnO) etched by diluted HCl effectively increases conversion efficiency of p-$Ni_{1-x}O$:Li/n-Si heterojunction solar cells. The results show that the short circuit current density (J_{sc}) of cell etched at 10 s increases about 8.5% compared to unetched cell, which also corresponds to the increase of efficient photoelectric conversion in NIR region as shown in external quantum efficiency spectra. It is attributed to the increase of light transmittance of AZOY thin films in the NIR region and the effective light path of the NIR wavelength, which results in increasing of light absorption in the base layer.

1. Introduction

A type of silicon heterojunction solar cell, called heterojunction with intrinsic thin-layer (HIT), developed by Sanyo Ltd., in 1994, offers low temperature (<250°C) process for high-efficiency solar cells compared to crystalline silicon solar cells with diffused p-n junctions. Today, the ultra-high conversion efficiency of 25.6% (area = 143.7 cm^2) has been achieved in HIT solar cell, April 2014. However, the cell still exhibits a high process cost and technical barriers because of its complex structure, despite the fact that it can be fabricated at a rather low temperature (<250°C) [1, 2]. By comparison, the low cost transparent conducting oxide (TCO)/n-Si heterojunction solar cells (HJSCs) are more promising as high-conversion-efficiency and low cost SCs because of the advantages they offer, including a simpler device structure and a lower processing temperature (<250°C) [3–13]. In 2013, our study [14] proposed that low cost p-type $Ni_{1-x}O$:Li thin film was a promising material candidate for other TCO materials (such as n-ZnO-base or n-type indium tin oxide (n-ITO)) in HJSCs applications due to the higher work function (>5 eV), which can directly increase the built-in potential (V_{bi}) and further increase the V_{oc}. However, the results show that the conversion efficiency of p-$Ni_{1-x}O$:Li/n-Si HJSCs is only 2.33% (V_{oc}: 345 mV, J_{sc}: 22.048 mA/cm^2, and FF: 0.307). We propose that the reduction of interface states (D_{it}) of cell and the improvement of optoelectrical properties of p-$Ni_{1-x}O$:Li thin films are very important issues to develop high conversion efficiency p-$Ni_{1-x}O$:Li/n-Si HJSC.

The low J_{sc} value of p-$Ni_{1-x}O$:Li/n-Si HJSCs is a serious problem to limit the conversion efficiency of cell. It is mainly attributed to high reflectance of n-Si substrate (~25%), low transmittance of p-$Ni_{1-x}O$:Li thin films (~50%), and light absorption loss of n-Si. Surface texturation of TCO thin films window layers by wet chemical etching is a simple and effective method to increase J_{sc}, which has been reported in many solar cells applications [15–18]. This method performs light scattering to increase the effective light path in a solar cell to enhance overall absorption. This is the so-called "light trapping." In fact, in these p-$Ni_{1-x}O$:Li/n-Si HJSCs, a high conductivity (high mobility) and dense Al-Y codoped ZnO (AZOY) thin film is deposited on p-$Ni_{1-x}O$:Li thin films as

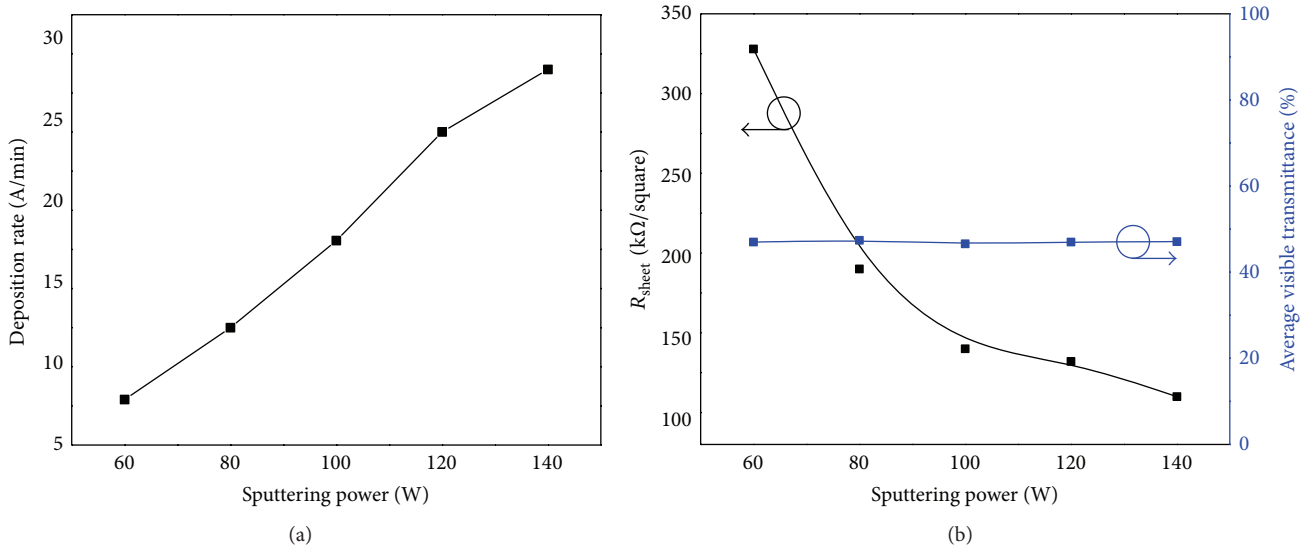

FIGURE 1: Dependence of (a) deposition rate and (b) sheet resistance (R_{sheet}) and average visible transmittance (400–800 nm) on the sputtering power for p-$Ni_{1-x}O$:Li thin films.

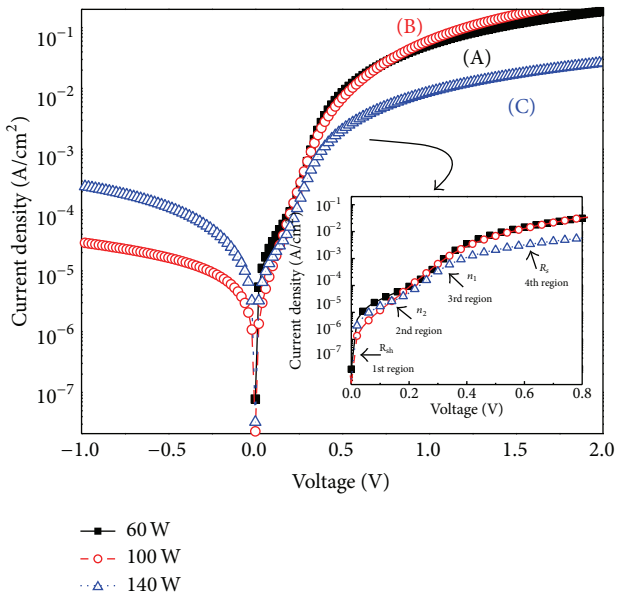

FIGURE 2: Dark current density-voltage (D*J*-*V*) curve of p-$Ni_{1-x}O$:Li/n-Si HJ fabricated at sputtering power of 60 W (line A), 100 W (line B), and 140 W (line C).

a front electrode contact layer (or called window layer). Thus, an appropriate postdeposition etching for AZOY thin film may increase J_{sc} of p-$Ni_{1-x}O$:Li/n-Si HJSCs.

In this study, the effects of sputtering power on the optoelectrical properties of p-$Ni_{1-x}O$:Li thin films were first investigated. And then, low cost p-$Ni_{1-x}O$:Li/n-Si HJSCs were fabricated, and wet chemical etching with diluted HCl was used to produce the AZOY surface texture. The effect of wet etching on film surface morphology and cell performance was also investigated.

2. Experiment

P-type Li-doped $Ni_{1-x}O$ (p-$Ni_{1-x}O$:Li) thin films were deposited on glass and n-type silicon (1 0 0) substrates with a resistivity of 1–10 Ωcm and a 250 μm thickness by RF magnetron sputtering with a 3-inch diameter NiO : Li_2O (98.5 : 1.5 wt.%, 99.9% purity) ceramic target. The glass substrates were first cleaned with standard cleaning procedures (acetone and methanol) in an ultrasonic bath for 10 min to remove grease and organic contaminations and then rinsed in deionized water. A turbo molecular pump reduced the base pressure to 2×10^{-6} Torr prior to deposition. In sputtering process, the working pressure was fixed at 4 mTorr in ambient Ar (6% O_2) and the films were deposited at room temperature (RT). In order to investigate the effects of the RF sputtering power on the optoelectrical properties of p-$Ni_{1-x}O$:Li thin films, the sputtering power was manipulated in the range of 60–140 W.

For p-$Ni_{1-x}O$:Li/n-Si HJSC fabrication, the n-Si substrates were first cleaned by standard RCA procedures. The optimal p-$Ni_{1-x}O$:Li thin film was then deposited on the n-Si substrate. After p-$Ni_{1-x}O$:Li thin films deposition, high conductivity Al-Y codoped ZnO (AZOY) thin film was deposited by using RF magnetron sputtering and the Al was thermally deposited onto the back surface of n-Si as a back electrode. And then, a finger-shaped Al layer served as the front electrode. To expose the surface texture, the as-grown AZOY thin films were dipped in a diluted mixture of HCl in H_2O (0.1 M HCl) at room temperature (etching rate: approximately 9 ± 0.1 nm/s). Finally, the cells area was fixed at 1 cm^2 by cutting four edges.

The electrical and optical properties of p-$Ni_{1-x}O$:Li thin films were measured by four point probes and UV-visible-NIR spectrophotometer (HITACHI U-4100), respectively. A field-emission scanning electron microscope (FE-SEM, JEOL-6700) was used to observe film surface morphology.

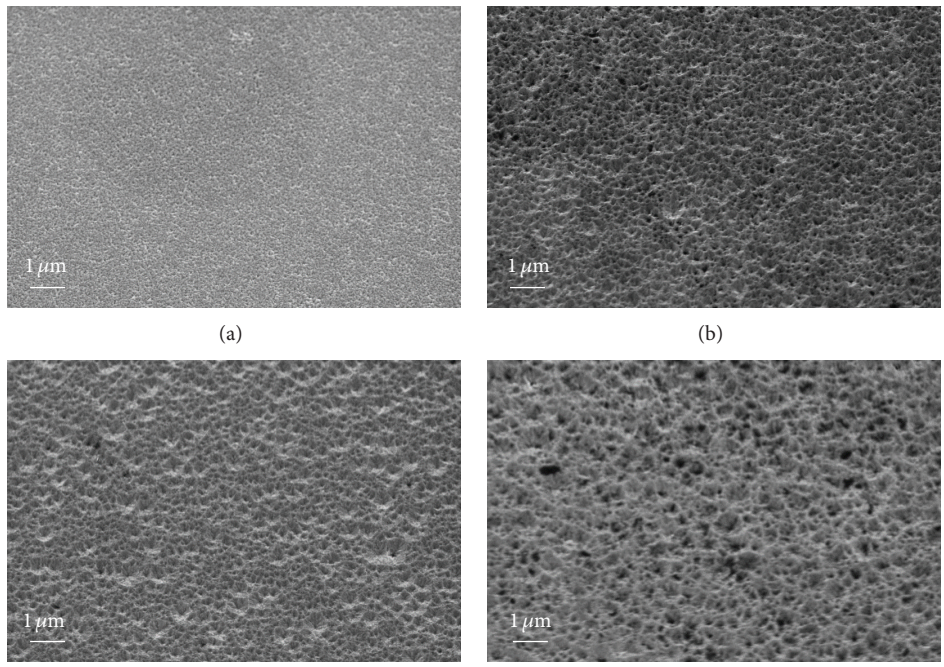

Figure 3: SEM micrographs (at 45° tilt) of AZOY thin films etched in 0.1 M HCl for (a) 0 s, (b) 10 s, (c) 20 s, and (d) 30 s.

The 3D images, line profiles, and surface root-mean-square (RMS) roughness of AZOY thin films were estimated by atomic force microscopy (AFM, BASO-SPM). The dark current density-voltage (J-V) characteristics of the device were measured by using an Agilent B 1500A semiconductor parameter analyzer. The photovoltaic characteristics of the device were tested using an AM 1.5 standard Newport #96000 solar simulator (Peccell PEC-L11) with an illumination intensity of 100 mW/cm^2. External quantum efficiency (EQE) measurements were tested by filtering the Xe lamp with a monochromator; the signal was collected by a merlin detector and preamplifier.

3. Results and Discussion

Figure 1(a) shows the dependence of the deposition rate of the p-$Ni_{1-x}O$:Li thin film on the sputtering power. A linear increase on growth rate was observed as the sputtering power increased. This indicates that the number of atoms sputtered from the target is proportional to the sputtering power. For higher sputtering power, the sputtered species get a higher energy that contributes to the film growth. These high energy particles have high surface mobility, and therefore a higher growing process at the surface takes place [19]. It also corresponds to electrical properties of p-$Ni_{1-x}O$:Li thin film as seen in Figure 1(b). Clearly, the sheet resistance of films decreases from 328 kΩ/square to 110 Ω/square as the sputtering power increases from 60 W to 140 W. The variations are from improved crystallinity and reduced grain boundary scattering to charge carriers as sputtering power increased. All of the effects lead to a decrease in the sheet resistance of the p-$Ni_{1-x}O$:Li thin film. In addition, there is no significant change in average visible transmittance (400–800 nm, ~47%) for all films. However, this value, compared to other TCO films (>75%), is still low, which can be attributed to the presence of Ni^{3+} in Ni_2O_3 acting as color centers in $Ni_{1-x}O$ films [20].

The dark current density-voltage (DJ-V) curve of p-$Ni_{1-x}O$:Li/n-Si HJSCs fabricated at sputtering power of 60 W, 100 W, and 140 W were shown in Figure 2. In this figure, the forward bias log J-V curve for lines A and C shows four linear regions and for line B shows three linear regions (the slope of 2nd region is similar to 3rd region), separated by transition segments. The slopes in 1st and 4th regions for line B imply that it has the highest R_{sh} and the lowest R_s. In addition, if the forward-biased curve is fitted to the standard diode equation, we find that the ideality factors for line A are 3.41 (2nd region) and 1.72 (for 3rd region) and for line B are 1.94 (2nd and 3rd region) and for line C are 3.55 (2nd region) and 1.99 (for 3rd region). The ideality factor close to 2 indicates that the forward current in 3rd region is mainly limited by recombination within the junction space charge region. In particular, lines A and C show a higher ideality factor at lower voltage level (2nd region). The forward current in 2nd region can be mainly explained using a trap-assisted interface recombination model, which is attributed to the recombination of electrons from n-Si with holes from p-$Ni_{1-x}O$:Li thin film, through interface states produce extra current [21, 22]. Moreover, it implies that more interface states are generated at the junction when the sputtering power is either extremely high or extremely low. This high interface

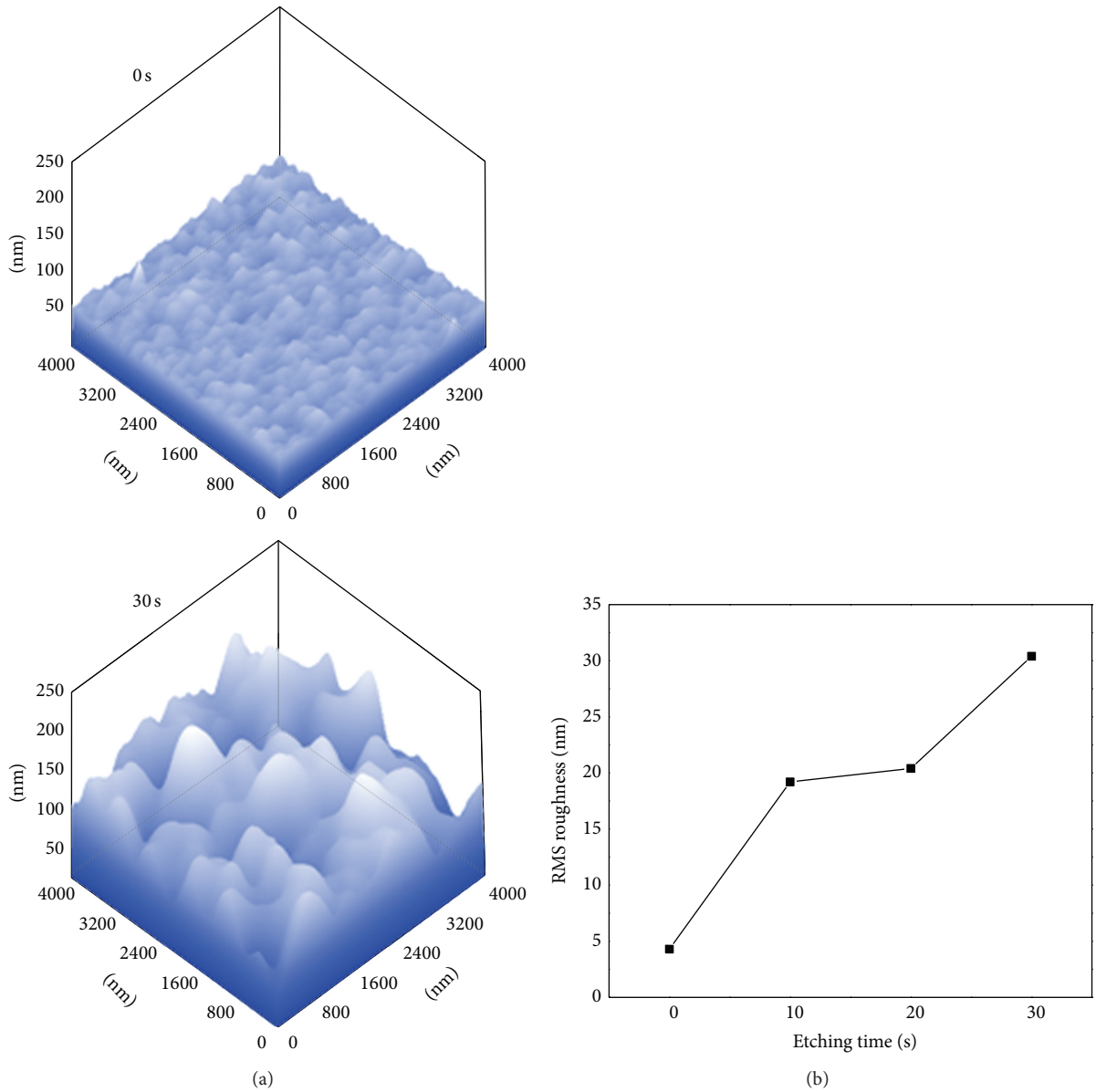

Figure 4: Surface RMS roughness of AZOY thin films as a function of etching time.

state can pin the Fermi level and change the V_{bi}; they also act as recombination centers that supply a shunt to the light-generated current. Thus, we determine that the sputtering power of 100 W is the best parameter in this study.

Figure 3 shows the surface morphology (at 45° tilt) of AZOY thin film before and after etching. Unetched AZOY surface reveals irregular polyhedral grains with smooth morphology. After etching, the surface morphology changes from smooth to lunar landscape-like with small angles. Figure 4 shows the surface RMS roughness of AZOY thin film etched in various periods. The surface RMS roughness increases with etching time, indicating that adjusting etching time affects AZOY thin-film surface roughness. The AZOY thin-film surface RMS roughness values are estimated as 4.3 ± 0.12 nm (0 s), 19.2 ± 0.18 nm (10 s), 20.4 ± 0.17 nm (20 s), and 30.4 ± 0.23 nm (30 s). This variation in surface morphology and surface RMS roughness may affect the optical properties of films and then influence the conversion efficiency of cell.

Figure 5 shows the optical properties of AZOY thin films deposited on glass substrate etched in various periods. A clear observed oscillation in unetched AZOY thin film (between 85% and 95%) is basically the Fabry-Perot interference [23, 24]. Along with the etching process, the oscillation phenomenon disappears gradually because of the rough surface. The average visible transmittance for all AZOY thin films is approximately 91%, indicating that AZOY thin films have good light transmittance for solar cell applications. Sharp fundamental absorption edge in near ultraviolet region was observed in all spectra, corresponding to energy band gap transition of ZnO. In addition, the transmittances become

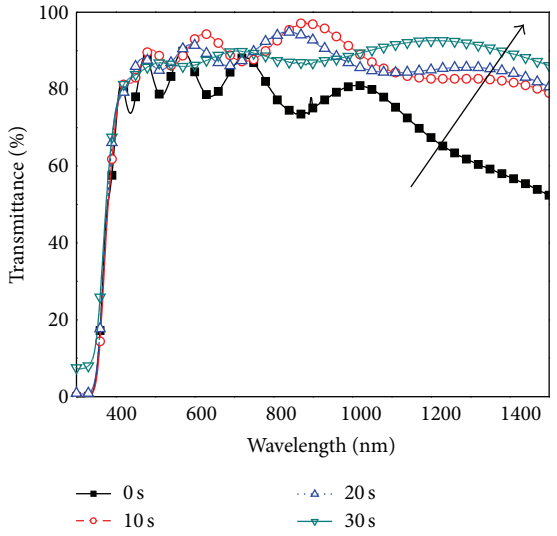

Figure 5: Optical transmittance of AZOY films etched in 0.1 M HCl for various etching times.

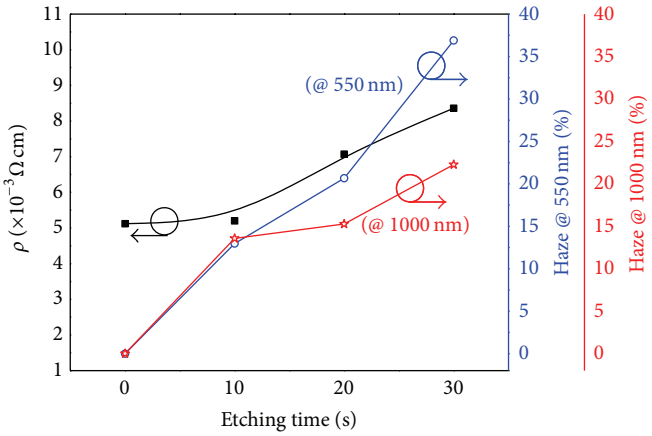

Figure 6: Dependence of electrical resistivity (ρ) and haze value at 550 nm and 1000 nm on the etching time for AZOY thin films.

higher in the near infrared ray (NIR) region as etching time increases. This shifting NIR wavelength is consistent with the carrier concentration changing with etching time variation [25, 26], which can be reasoned from electrical resistivity (ρ) of AZOY thin films (Figure 6). The unetched AZOY thin film has the lowest electrical resistivity of 5.12×10^{-3} Ωcm. With an increase in etching time, the resistivity of the AZOY thin film gradually increases to 8.36×10^{-3} Ωcm. The electrical resistivity is related to carrier concentration (n) through the carrier mobility (μ):

$$\rho = \frac{1}{qe\,\mu}. \tag{1}$$

Therefore, this variation trend in resistivity may be reasoned as follows: (i) larger effective surface areas cause oxygen adsorption to trap carriers or form film defects, which results in resistivity variation. Also, the larger effective surface area affects carrier motions due to the shortened conduction path of carriers. (ii) The grain boundary of AZOY thin film deteriorated at long etching time and formed more defect sites (areas) throughout the whole boundary [27]. These defect sites result in an increase in carrier scattering and a decrease in carrier mobility. Therefore, AZOY thin film conductivity decreases with an increase in etching time. Based on the results, the decrease of conductivity of window layer leads to an increase of the lateral resistance, which will directly increase the series resistance (R_s) of cell. The haze values at 550 nm and 1000 nm of AZOY thin films etched at various etching times are also shown in Figure 6 and it is concluded that, by using (2) [18, 27],

$$\text{Haze} = \frac{T_{\text{diffuse}}}{T_{\text{total}}}, \tag{2}$$

where T_{total} is the total transmittance and T_{diffuse} is the diffuse transmittance. For the unetched AZOY thin film,

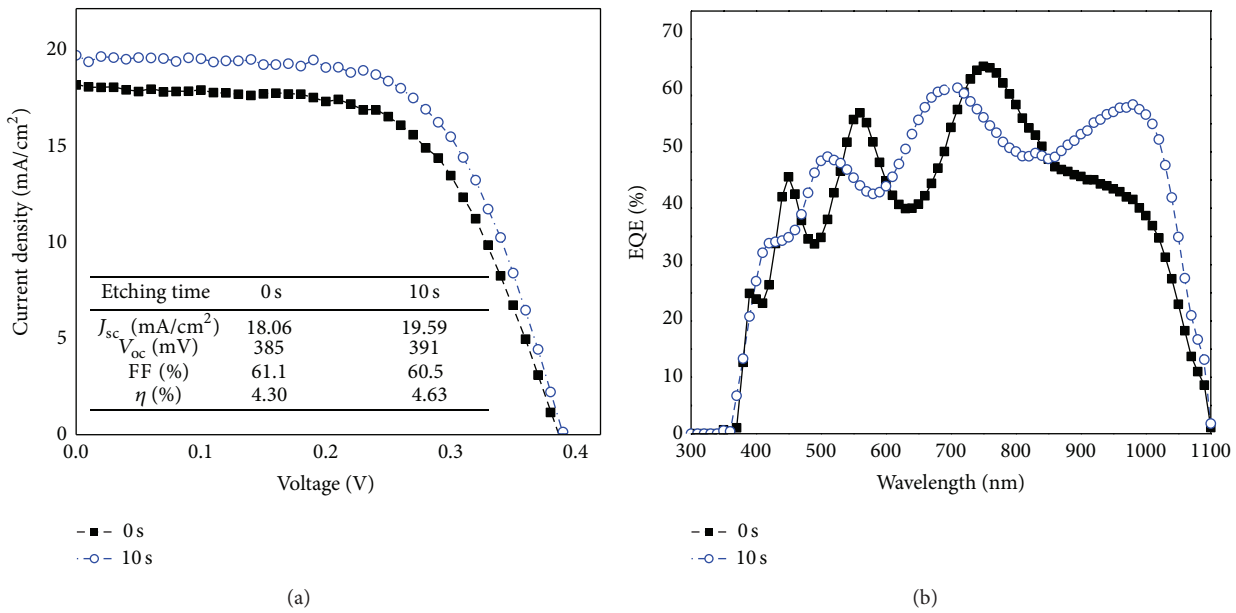

FIGURE 7: Photoelectric effect measurement of p-$Ni_{1-x}O$:Li/n-Si HJSC before and after being etched for 10 s for (a) L*J-V* and (b) EQE.

the haze value is approximately 0%, indicating that disorderly polyhedral grains with smooth morphology cannot produce light scattering. After postdeposition etching, the AZOY thin film haze values increase to aid the increase in diffuse transmittance and the effect of light trapping becomes more and more obvious. This shows that surface roughness affects light scattering, especially for different lateral feature sizes.

The results show that the increase in etching time affects the series resistance (R_s) effect (conductivity loss) and increases the light trapping effect (haze value increase) for p-$Ni_{1-x}O$:Li/n-Si HJSC applications. This implies that the etching time of 10 s and 20 s should be the best choice. However, for etching time of 20 s, a very poor photovoltaic properties of cell are obtained (conversion efficiency of ~0%). This is probably because of the "through-etching" occurring earlier, due to different substrates. Therefore, we will only compare the cell before and after 10 s etching. Figure 7 shows the L*J-V* curve and EQE spectra of an p-$Ni_{1-x}O$:Li/n-Si HJSC before and after 10 s etching. It shows that the J_{sc} of cell etched at 10 s increases about 8.5% compared to unetched cell. This increase of J_{sc} also corresponds to the increase of efficient photoelectric conversion in NIR region as seen in EQE spectra, which can be reasoned as the follows. (i) The light transmittance of AZOY thin films in the NIR region increases; thus, the NIR absorption in the base layer increases. (ii) Haze value affects the amount of light scattering; therefore, the effective light path of the NIR wavelength increases as the light absorption in the base layer increases. Because of these two reasons, more electron-hole pairs are formed and collected, resulting in increase of J_{sc}. Therefore, it is confirmed that wet etching in a short time is a simple and effective method to increase J_{sc} in solar cell applications.

4. Conclusion

This study successfully fabricates low cost p-$Ni_{1-x}O$:Li/n-Si HJSC using RF magnetron sputtering. From D*J-V* curve, more interface states are generated at the junction when the sputtering power is either extremely high or extremely low. The results show that the sputtering power of 100 W is the best parameter in this study. SEM images show that AZOY thin film surface morphology changes from smooth to cratered, resulting in an increase in surface RMS roughness. The haze spectra show that surface roughness affects light scattering properties. The EQE of cells in the NIR region increases as the etching time increases, which corresponds to the J_{sc} of cell etched at 10 s increases about 8.5% (from 18.06 to 19.59 mA/cm^2) compared with unetched cell.

Conflict of Interests

The authors declare that there is no conflict of interests regarding the publication of this paper.

Acknowledgment

The authors gratefully acknowledge the financial support from the National Science Council of Taiwan (Grant nos. NSC-102-2221-E-006-242-MY2 and MOST 103-2221-E-230-019).

References

[1] M. Taguchi, K. Kawamoto, S. Tsuge et al., "HITTM cells—high-efficiency crystalline Si cells with novel structure," *Progress in Photovoltaics*, vol. 8, pp. 503–513, 2000.

[2] Y. Tsunomura, Y. Yoshimine, M. Taguchi et al., "Twenty-two percent efficiency HIT solar cell," *Solar Energy Materials & Solar Cells*, vol. 93, no. 6-7, pp. 670–673, 2009.

[3] J. C. Manifacier and L. Szepessy, "Efficient sprayed In_2O_3: Sn n-type silicon heterojunction solar cell," *Applied Physics Letters*, vol. 31, no. 7, pp. 459–462, 1977.

[4] F.-H. Hsu, N.-F. Wang, Y.-Z. Tsai, and M.-P. Houng, "A novel Al and Y codoped ZnO/*n*-Si heterojunction solar cells fabricated by pulsed laser deposition," *Solar Energy*, vol. 86, no. 11, pp. 3146–3152, 2012.

[5] H.-W. Fang, T.-E. Hsieh, and J.-Y. Juang, "Influences of SiO_x layer thickness on the characteristics of In-Zn-O/SiO_x/*n*-Si hetero-junction structure solar cells," *Surface and Coatings Technology*, vol. 231, pp. 214–218, 2013.

[6] H. Kobayashi, S. Tachibana, K. Yamanaka, Y. Nakato, and K. Yoneda, "Improvement of "indium-tin-oxide/silicon oxide/*n*-Si" junction solar cell characteristics by cyanide treatment," *Journal of Applied Physics*, vol. 81, no. 11, pp. 7630–7634, 1997.

[7] O. Malik, F. J. de la Hidalga-W, C. Zúñiga-I, and G. Ruiz-T, "Efficient ITO-Si solar cells and power modules fabricated with a low temperature technology: results and perspectives," *Journal of Non-Crystalline Solids*, vol. 354, no. 19–25, pp. 2472–2477, 2008.

[8] D. Song, A. G. Aberle, and J. Xia, "Optimisation of ZnO:Al films by change of sputter gas pressure for solar cell application," *Applied Surface Science*, vol. 195, no. 1–4, pp. 291–296, 2002.

[9] F.-H. Hsu, N.-F. Wang, Y.-Z. Tsai, M.-C. Chuang, Y.-S. Cheng, and M.-P. Houng, "Study of working pressure on the opto-electrical properties of Al-Y codoped ZnO thin-film deposited using DC magnetron sputtering for solar cell applications," *Applied Surface Science*, vol. 280, pp. 104–108, 2013.

[10] H. Iimoiri, S. Yamane, T. Kitamura, K. Murakoshi, A. Imanishi, and Y. Nakato, "High photovoltage generation at minority-carrier controlled n-Si/p-CuI heterojunction with morphologically soft CuI," *The Journal of Physical Chemistry C*, vol. 112, no. 30, pp. 11586–11590, 2008.

[11] N. Gupta, R. Singh, F. Wu et al., "Deposition and characterization of nanostructured Cu_2O thin-film for potential photovoltaic applications," *Journal of Materials Research*, vol. 28, no. 13, pp. 1740–1746, 2013.

[12] F. Gao, X.-J. Liu, J.-S. Zhang, M.-Z. Song, and N. Li, "Photovoltaic properties of the p-CuO/n-Si heterojunction prepared through reactive magnetron sputtering," *Journal of Applied Physics*, vol. 111, no. 8, Article ID 084507, pp. 084507-1–084507-4, 2012.

[13] K. V. Rajani, S. Daniels, M. Rahman, A. Cowley, and P. J. McNally, "Deposition of earth-abundant p-type CuBr films with high hole conductivity and realization of p-CuBr/n-Si heterojunction solar cell," *Materials Letters*, vol. 111, pp. 63–66, 2013.

[14] F. H. Hsu, N. F. Wang, Y. Z. Tsai, Y. S. Cheng, and M. P. Houng, "A new p-$Ni_{1-x}O$: Li/n-Si heterojunction solar cell fabricated by RF magnetron sputtering," *Journal of Physics D: Applied Physics*, vol. 46, no. 27, Article ID 275104, 2013.

[15] M. Berginski, J. Hüpkes, M. Schulte et al., "The effect of front ZnO:Al surface texture and optical transparency on efficient light trapping in silicon thin-film solar cells," *Journal of Applied Physics*, vol. 101, no. 7, Article ID 074903, 2007.

[16] J. Springer, B. Rech, J. Müller, and M. Vanecek, "TCO and light trapping in silicon thin film solar cells," *Solar Energy*, vol. 77, no. 6, pp. 917–930, 2004.

[17] P. A. Basore, "Numerical modeling of textured silicon solar cells using PC-1D," *IEEE Transactions on Electron Devices*, vol. 37, no. 2, pp. 337–343, 1990.

[18] N.-F. Wang, Y.-Z. Tsai, and F.-H. Hsu, "Effect of surface texture on Al-Y codoped ZnO/n-Si heterojunction solar cells," *IEEE Transactions on Electron Devices*, vol. 60, no. 12, pp. 4073–4078, 2013.

[19] X. Yu, J. Ma, F. Ji et al., "Effects of sputtering power on the properties of ZnO:Ga films deposited by r.f. magnetron-sputtering at low temperature," *Journal of Crystal Growth*, vol. 274, no. 3-4, pp. 474–479, 2005.

[20] Y. Zhou, D. Gu, Y. Geng, and F. Gan, "Thermal, structural and optical properties of NiO_x thin films deposited by reactive dc-magnetron sputtering," *Materials Science and Engineering B: Solid-State Materials for Advanced Technology*, vol. 135, no. 2, pp. 125–128, 2006.

[21] S. Majumdar and P. Banerji, "Temperature dependent electrical transport in *p*-ZnO/*n*-Si heterojunction formed by pulsed laser deposition," *Journal of Applied Physics*, vol. 105, no. 4, Article ID 043704, 2009.

[22] R. K. Gupta, K. Ghosh, and P. K. Kahol, "Fabrication and characterization of NiO/ZnO p-n junctions by pulsed laser deposition," *Physica E: Low-Dimensional Systems and Nanostructures*, vol. 41, no. 4, pp. 617–620, 2009.

[23] J. Zhu, C.-M. Hsu, Z. Yu, S. Fan, and Y. Cui, "Nanodome solar cells with efficient light management and self-cleaning," *Nano Letters*, vol. 10, no. 6, pp. 1979–1984, 2010.

[24] T. Dhakal, A. S. Nandur, R. Christian et al., "Transmittance from visible to mid infra-red in AZO films grown by atomic layer deposition system," *Solar Energy*, vol. 86, no. 5, pp. 1306–1312, 2012.

[25] J. L. Zhao, X. W. Sun, H. Ryu, and Y. B. Moon, "Thermally stable transparent conducting and highly infrared reflective Ga-doped ZnO thin films by metal organic chemical vapor deposition," *Optical Materials*, vol. 33, no. 6, pp. 768–772, 2011.

[26] H. Kim, A. Piqué, J. S. Horwitz et al., "Effect of aluminum doping on zinc oxide thin films grown by pulsed laser deposition for organic light-emitting devices," *Thin Solid Films*, vol. 377-378, pp. 798–802, 2000.

[27] W. T. Yen, Y. C. Lin, and J. H. Ke, "Surface textured ZnO:Al thin films by pulsed DC magnetron sputtering for thin film solar cells applications," *Applied Surface Science*, vol. 257, no. 3, pp. 960–968, 2010.